Bimodal argon ion velocity distribution functions downstream of an expanding helicon source plasma

I. A. Biloiu[1], E. E. Scime[1], C. Biloiu[2], and S. A. Cohen[3]

[1] *West Virginia University, Physics Department, Morgantown, WV 26506, USA*
[2] *Varian Semiconductor Equipment Associates, 35 Dory Road, Gloucester, MA 01930, USA*
[3] *Princeton Plasma Physics Laboratory, Princeton, NJ 08543, USA*

Bimodal ion velocity distribution functions along diverging magnetic field lines have been observed via laser induced fluorescence downstream from the helicon source-diffusion chamber junction in the HELIX-LEIA device. By decreasing the magnetic field in the diffusion chamber, i.e., by increasing the magnetic field gradient in the expansion region, the speed of the faster component of the distribution function increases, reaching a maximum of ~ 10 km/s. The speed of the slower component is essentially unchanged. Although the total metastable ion population detected by laser induced fluorescence decreases as the gradient of the magnetic field increases, the ratio of the amplitude of fast component to the slow component increases exponentially from ~0.4 to ~1.7 as the LEIA magnetic field decreases from 70 G to 7 G.

1. Introduction

Recently, a new phenomenon – formation of a current-free electric double layer (EDL) at the end of a helicon plasma source, in a region of divergent magnetic field and for pressures below a threshold value, has garnered considerable interest in the plasma physics community [1-4]. Since the EDL is oriented with the high potential side toward the helicon source, ions are accelerated out of the helicon source into the expansion. Observations of ion speeds larger than a few times the ion sound speed make this phenomenon of interest for ion thrusters and plasma processing. Although many experimental, modelling, and theoretical reports [5-7] have managed to clarify aspects of the EDL formation process, some questions remain. For example, through which external control parameters can the EDL strength, thickness, and shape be varied? What is the role of the magnetic field profile in EDL formation and strength?

The measurable parameter of interest in studies of EDL physics is the ion velocity (energy) distribution function before and after the ions pass through the EDL. One method for obtaining the ion velocity distribution function (ivdf) in plasma is laser induced fluorescence (LIF). Unlike the retarding field energy analyzer (RFEA) method, which requires energy corrections for the perturbation to the ivdf by the sheath created in the front of the RFEA, LIF is non-intrusive. Furthermore, since the ion absorption linewidth is much larger than probing laser line width (roughly tenfold for dye lasers and one thousand times for diode lasers), high resolution measurements of bulk velocity and temperature can be obtained. LIF also has a high spatial resolution, usually few mm^3, defined by the intersection of the probe laser with the optical collection path. The main drawback of LIF is that the inferred ivdf reflects the population of a certain excited state (for instance, for the 3 level LIF scheme $3d'\ ^2G_{9/2} \rightarrow 4p'\ ^2F_{7/2} \rightarrow 4s'\ ^2D_{5/2}$ usually employed for Ar II investigations, it is the metastable state $3d'\ ^2G_{9/2}$) and not the entire ion population. However, it has been shown that for this Ar II state, in low pressure helicon plasma, the main population mechanism is excitation by electron impact from the

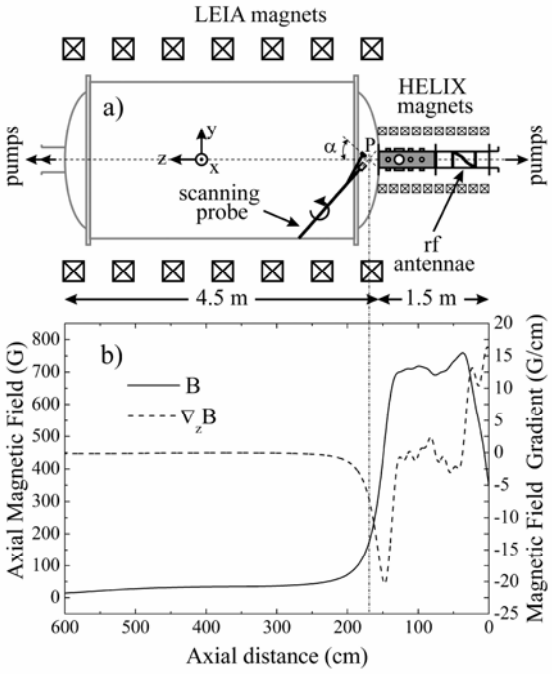

FIG. 1. a) HELIX-LEIA helicon source - diffusion chamber system; b) the magnetic field profile and the magnetic field gradient on the axis of the system.

ion ground state. Under these conditions, the population of the $3d'\ ^2G_{9/2}$ metastable level is proportional to $n^2T_e^{1/2}$ (n-plasma density, T_e-the electron temperature) [3]. Although not absolutely calibrated, this scaling law provides a qualitative correlation between the LIF signal and the total ion density.

We report new measurements of ivdfs in EDLs for various magnetic field gradients in the helicon source-diffusion chamber expansion region. The parallel ivdf has a bimodal structure with a slow ion group practically at rest and a fast ion group having speeds as high as ~2.4 c_s ($c_s = (k_BT_e/m)^{1/2}$, the ion sound speed). The perpendicular ivdf is a single distribution. By decreasing the magnetic field in the expansion region, i.e., increasing the magnetic field gradient, both the speed of the fast component and the fast/slow population ratio increase.

2. Experimental

2.1. Helicon plasma source

The helicon plasma source used for these investigations has been described in detail elsewhere [3]. The essential characteristics of the HELIX-LEIA machine are as follows: HELIX (Hot hELIcon EXperiment) consists of a 61 cm long, 10 cm diameter Pyrex tube mated to a 91 cm long, 15 cm diameter stainless steel tube (see Fig. 1a). Ten electromagnets produce a magnetic field of 0-1.2 kG along the tube axis. A 19 cm long, $m = +1$, helical antenna couples rf energy into the plasma. A rf amplifier furnishes up to 2 kW over a frequency range of 6-18 MHz. The plasma produced in the source expands into a 4.5 m long 2 m diameter diffusion chamber, LEIA (Large Experiment on Instabilities and Anisotropies). The LEIA chamber is surrounded by 7 electromagnets that provide an axial magnetic field of up to 150 G. There is an axial magnetic field gradient in the region between the helicon source and the expansion chamber that peaks at the throat of the source (see Fig. 1b).

2.2. Laser induced fluorescence diagnostic

Simultaneous measurements of electron temperature, electron density, plasma potential, magnetic fluctuation spectrum in three dimensions, and the two dimensional ivdf in LEIA were obtained with an internal, scanning LIF probe (see [8] for details of the probe). Probe measurements are made throughout a horizontal plane 100 cm in length along the z-axis and 40 cm wide in the radial direction. All measurements in this work were obtained in the divergent magnetic field region 19 cm downstream from the HELIX-LEIA junction

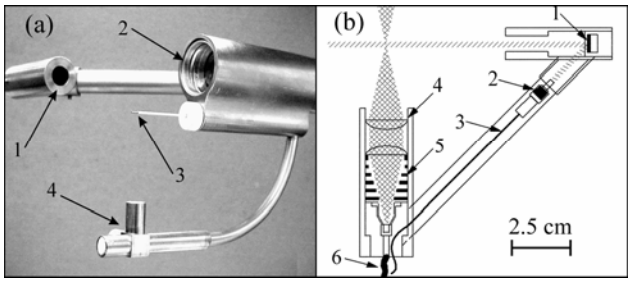

FIG. 2. Scanning probe: (a) 1–LIF injection optics; 2–LIF collection optics; 3–rf compensated Langmuir probe; 4–3D magnetic sense coil array. (b) 1–injection mirror; 2–collimating injection optic; 3–injection fiber; 4–collection lens; 5–light baffles; 6–collection fiber.

(point P in Fig. 1). The diagnostic complement mounted on the probe head (Fig. 2a) includes: LIF optics, a rf compensated cylindrical Langmuir probe and a 3D magnetic sense coil array. For Ar II LIF, laser light pumps the Ar II $3d^2G_{9/2}$ metastable state to the $4p^2F_{7/2}$ state, which then fluoresces by emitting 460.96 nm photons. To measure the full ivdf, the laser (Coherent 899 ring dye laser with rhodamine 6G dye pumped by a 6 W Innova 90 argon-ion laser) frequency is swept over 20 GHz. The injected laser power density was ~ 11 mW/mm^3, i.e., the LIF was operated in linear regime [9]. During each scan of the laser, 10% of the laser light is passed through an iodine cell and the iodine fluorescence recorded. The molecular iodine spectrum provides a means of compensating for laser drift and measuring the absolute velocity of the argon ions. The Ar II bulk flow velocity is obtained from the Doppler shift in the fluorescence spectrum

$$\lambda_0 \Delta\nu_D \cong \boldsymbol{V}\boldsymbol{k}_{\boldsymbol{L}} \qquad (1)$$

where λ_0 is the rest frame absorption wavelength, $\Delta\nu_D$ is the Doppler shift of the absorption line, $\boldsymbol{V}$ is the particle velocity, and $\boldsymbol{k}_{\boldsymbol{L}}$ the laser propagation direction. Zeeman corrections may be added to $\Delta\nu_D$, but since the magnetic field strength at the observation point is low (~210-280 G) for these measurements, the Zeeman split between σ^+ and σ^- components is estimated to be ~0.9 GHz<<~9 GHz (the distribution width) and is therefore neglected.

3. Bimodal parallel ivdfs

As previously reported [1-6], the EDL strength in helicon plasma scales with gas pressure: the EDL appears below a threshold value of 1-2 mTorr and the potential drop across the EDL increases as the pressure decreases. However, as the plasma density decreases, the LIF signal/noise ratio (SN) worsens. To ensure adequate LIF SN with moderate EDL strength, these measurements were made at an ope-

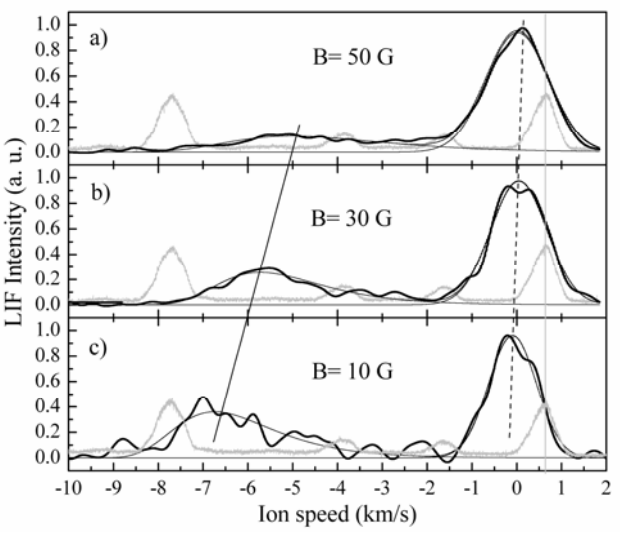

FIG. 3. Bimodal ivdfs obtained for different magnetic fields in the diffusion chamber: a) B=50 G; b) B=30 G; c) B=10 G. The distributions are normalized to peak of the slow population. Shown in the figure are the raw LIF signal (thick black line); a fit to the ivdfs (thin black line); iodine reference spectrum (thin grey line); the iodine reference line (grey vertical line); the center of the slow ion population (dashed vertical line), and the center of the fast ion population (oblique straight line).

rating pressure of 1.5 mTorr; input power 800 W; rf frequency 9.5 MHz; and magnetic field in the source of 600 G. The signature of EDL formation is a bi-modal parallel ivdf comprised of a fast and a slow ion population. Present understanding is that these two populations have different origins: the slow ions are a background population created in the expansion region and the fast ions are accelerated by the EDL from the source into the diffusion chamber.

Previous studies have shown that in helicon discharges the EDL appears near the source-diffusion chamber junction where the magnetic field gradient is largest. *Charles* [10] reported that EDL formation in the Chi-Kung helicon source is triggered by the magnetic field profile and strength in the source; below a threshold value of the magnetic field in the source the EDL doesn't form. For the same source, *Keesee et al.* [11] reported that EDL potential drop scales with magnetic field strength in the source: the fast ion parallel flow speed increased from 2.5 km/s to 5 km/s as the magnetic field increased from 50 G to 140 G. No change in the fast ion flow speed was observed when the magnetic field profile at the end of the source was varied. *Nakano et al*. [12] showed that the ivdf structure is dependent on the magnetic configuration. For a mirror configuration, the parallel ivdf in the diffusion region of a helicon source has a bimodal structure with a slow component formed by local ionization and a fast

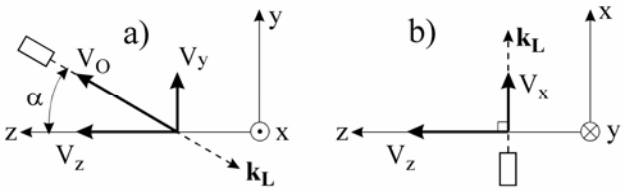

FIG. 4. Injection geometries for finding the true axial ion flow speed v_z. a) the laser is injected in the *yz* plane at an angle α relative to *z* direction ; b) the laser is injected in the *xz* plane along the *x* direction.

component drifting from a region of higher potential. A double cusp magnetic configuration eliminated the fast component. In the mirror configuration MNX source, *Cohen et al.* showed that within the mirror the ions have a subthermal axial drift [1]. Outside the mirrors coils, a supersonic fast ion population appears at low pressure. Also in MNX, *Sun et al.*[13] showed that contrary to expectations for a Laval-nozzle magnetic configuration, the fast ion speed decreases as the nozzle magnetic field is increased. All these observations indicate a strong correlation between the magnetic field profile, magnetic field strength and the EDL potential drop.

In HELIX, the magnetic field profile is fixed and only the total strength can be varied. When the magnetic field strength was varied in the source, there was no effect on the speed of ions in the diffusion chamber. However, when the magnetic field in the source was kept constant and the magnetic field in the diffusion chamber decreased, a significant increase in the speed of the fast component was observed (oblique straight line in Fig. 3). The speed of the slow population was unchanged (dashed line). These results are consistent with the MNX observations, i.e., an increase of the speed of the fast component as a nozzle-type magnetic field decreases and a nearly stationary Maxwellian velocity distribution for the slow component [13]. While the slow group is well fit with a single Gaussian distribution, the fast group has a long tail towards slower speeds; symptomatic of fast ions slowed down by charge exchange and/or elastic collisions with the background gas. Note that the speeds shown in Fig. 3 are raw data and must still be corrected for the injection angle (α) of the interrogating laser beam. The LIF intensity of the observed particle velocity when the laser is injected in an arbitrary $\xi\zeta$ plane at an angle θ relative to the ζ direction is given by [14]

$$I_\theta(V_O) = const. \iint f(v_\xi, v_\zeta) dv_\xi dv_\zeta \qquad (2)$$

where V_O is the observed velocity, v_ξ and v_ζ are the particle velocities along the ξ and ζ directions respectively. The integration range is given by the

Doppler resonance condition. From the geometry of Fig. 4a and Eq. (1),

$$V_O = -v_z \cos\alpha - v_y \sin\alpha \qquad (3)$$

To determine the true v_z, the probe is rotated around its axis by 90° and the laser injected along the x axis to measure v_x.

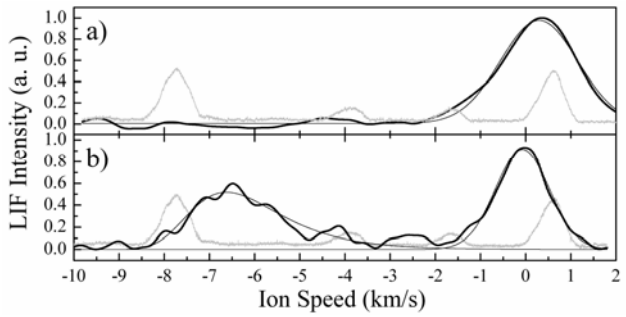

FIG. 5. Determination of the true parallel velocity of the fast ion population: a) LIF signal for the laser along x; b) LIF signal for the laser in the zy plane.

As shown in Fig. 5a, all the ions have a bulk v_x (perpendicular) speed of ~ 0 m/s. By cylindrical symmetry, v_y ~ 0 m/s. Thus, the true value of v_z for the fast group is given be $V_O/\cos\alpha$. The angle α for the point P in Fig. 1 was 26°. The thermal anisotropy of the slow group ivdf shown in Fig. 5 is partly an artifact of the diagnostic method and partly a fast population effect. For a thermally broadening ivdf measured along an arbitrary direction, the corresponding Doppler width is a Gaussian with an amplitude, center, and width that depend on the probe laser angle θ [11]. For our geometry, the correct parallel ion temperature is given by

$$k_B T_z = m(\Delta_{1/2} V_O)^2 / (8 \ln 2 \cos^2\alpha) \qquad (4)$$

where $\Delta_{1/2} V_O$ is the full width at half maximum of the measured ivdf.

The corrected v_z for the slow and fast ions versus LEIA magnetic field are shown in Fig. 6. Except for two points at very low magnetic field, the slow ions are practically at rest. The fast ion speed increases sharply as the magnetic field decreases and plateaus for LEIA magnetic fields below 30-40 G. At the lowest magnetic field strength of 7 G, the fast ion speed is supersonic $v_z \cong 2.4\ c_s$. The intensity of the fast ions relative to the slow ions also increases, from about 0.35 at 70 G up 1.71 at 7 G. The corrected parallel ion temperature of 0.13 eV for the slow ions is consistent with a background ion population heated by charge-exchange with fast ions. The measurements were restricted to LEIA fields below 70 G; at higher fields the fast ion LIF intensity is indistinguishable from the background.

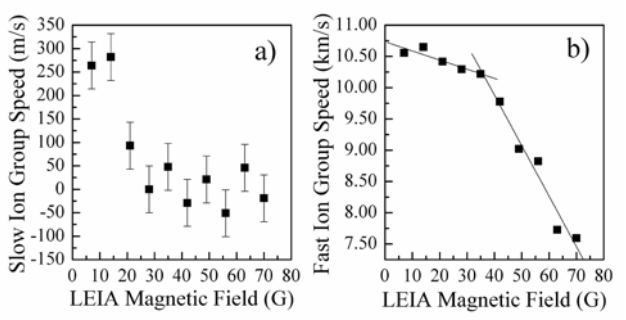

FIG. 6. Corrected flow speeds of the a) slow ion population and b) fast ion population as a function of LEIA magnetic field.

In a recently proposed model for EDL formation, *Chen* [15] assumed that the plasma is frozen to the magnetic field lines and that the plasma density and the magnetic field in the expansion region, relative to the source plasma, scale with the square of the plasma radius. According to this model, the ion fast kinetic energy cannot exceed ~ $5k_BT_e$. For our local electron temperature of 6 eV, the measured fast ion energy of ~ 23 eV is below the predicted 30 eV limit. The smaller fast ion energy may indicate energy losses due to heating the background gas through collisions. For the gas pressures used here, fast ions travelling from the source through the EDL are expected to experience 3-4 collisions before reaching the observation point [16].

3. References

[1] S. A. Cohen *et al.*,Phys. Plasmas **10** (2003) 2593.

[2] C. Charles and R. W. Boswell, Appl. Phys. Lett. **82** (2003) 1356

[3] X. Sun, C. Biloiu, R. Hardin, and E. Scime, Plasma Sources Sci. Technol. **13** (2004) 359

[4] N. Plihon, C. S. Corr, and P. Chabert, Appl. Phys. Lett. **86** (2005) 091501

[5] O. Sutherland, C. Charles, N. Plihon, and R. W. Boswell, Phys. Rev. Lett. **95** (2005) 2050002

[6] X. Sun *et al.*, Phys. Rev. Lett. **95** (2005) 025004

[7] M.A. Lieberman and C. Charles, Phys. Rev. Lett. **97** (2006) 045003

[8] C. Biloiu *et al.*, Rev. Sci. Instrum. **75 (**2004) 4296

[9] I. A. Biloiu, X. Sun, and E. E. Scime, Rev. Sci. Instrum. **77** (2006) 10F301

[10] C. Charles, Phys. Plasmas **12** (2005) 044508

[11] A. Keesee *et al.*, Phys. Plasmas **12** (2005) 093502

[12] T. Nakano *et al.*, J. Vac. Sci. Technol. B **11** (1993) 2046

[13] X. Sun *et al.*, Phys. Plasmas **12** (2005) 103509

[14] W. M. Ruyten, AIAA Journal **31** (1993) 2083

[15] F. F. Chen, Phys. Plasmas **13 (**2006) 101904

[16] C. Biloiu *et al.*, Plasma Sources Sci. Technol. **14** (2005) 359